Journal of Solid State Chemistry **149,** 236–241 (2000)
doi:10.1006/jssc.1999.8519, available online at http://www.idealibrary.com on IDEAL®

A New Bismuth–Selenium Oxychloride, $BiSeO_3Cl$: Crystal Structure and Dielectric and Nonlinear Optical Properties

P. S. Berdonosov,[1] S. Yu. Stefanovitch, and V. A. Dolgikh

Chemical Department, Moscow State University, 119899, GSP-3, Moscow, Russia

Received April 23, 1999; in revised form September 14, 1999; accepted September 21, 1999

A new oxychloride, $BiSeO_3Cl$, is obtained at 300°C from a mixture of BiOCl and SeO_2 as large colorless crystals. Room-temperature single-crystal X-ray investigation combined with an SHG test point to a noncentrosymmetric structure (space group $P2_12_12_1$, $a = 6.353(2)$, $b = 7.978(3)$, $c = 8.651(4)$ Å, $Z = 4$, $RF = 5.60\%$). The structure is characterized by a three-dimensional framework which is built up of BiO_5Cl_2 pentagonal bipyramids and trigonal pyramids of SeO_3E (E is the lone electron pair of Se(IV)). The dielectric and optical nonlinear properties of $BiSeO_3Cl$ are evaluated. © 2000 Academic Press

INTRODUCTION

In the past ten years a number of new substances with noncentrosymmetric structures were prepared in the systems $BiHal_3$–Bi_2O_3–TeO_2 and $LnOHal$–TeO_2, where Hal = Cl, Br, and I and Ln = rare earth elements, and their crystal structures were studied (1–5). The portion of noncentrosymmetric structures in these systems is relatively high (more than 40%). Many substances in these systems are related to so-called Sillen phases. The Sillen phases contain triple fluorite-like layers $[M_3O_x]$, where M = Bi (or Ln) and Te, while the x value depends on Te content. These triple layers are separated by the halogen atom layers. The principles of the formation of noncentrosymmetric structures in this class of substances were formulated in (5).

Information about similar oxychlorides containing bismuth and selenium is absent in the literature. In this work we present the results of syntheses of first representatives of Bi–Se oxychlorides, the crystal structure for noncentrosymmetric compound, and on investigation of its properties.

EXPERIMENTAL

Synthesis

Two new oxychlorides were found in a reaction mixture of BiOCl and SeO_2 (2 : 1) in an evacuated (10^{-2} Torr) quartz ampoule after annealing at 300°C, 240 h. BiOCl was prepared by boiling $BiCl_3 \cdot H_2O$ solution in distilled water for 3 h. The BiOCl precipitate was dried at 100–105°C after filtration. SeO_2 was prepared by oxidation of ultrapure Se in a stream of oxygen and nitrogen oxides. Reaction mixtures were prepared in a dry camera in an atmosphere of nitrogen, in order to avoid a reaction between selenium oxide and atmosphere water, and then were treated as described above. The formation of two types of crystals was observed in the ampoules.

The crystals of one type were plates of red color while others were colorless and large (up to 5–8 mm in size) with well-formed faces. X-ray local spectral analysis (Micro Analyzer CAMEBAX, PbSe and BiOCl single crystals as standards) showed the red crystals to be of $Bi_3Se_2O_7Cl_3$ ($3BiOCl \cdot 2SeO_2$) composition and the colorless crystals to be of $BiSeO_3Cl$ ($BiOCl \cdot SeO_2$) composition.

X-ray diffraction patterns for $BiSeO_3Cl$ (Enraf-Nonius, FR-552, Cu$K\alpha$1, Ge as internal standard) justified its crystallization in an orthorhombic system with lattice constants $a = 6.353(2)$, $b = 7.978(3)$, $c = 8.651(4)$ Å. When tested with the optical Second Harmonic Generation (SHG) technique by method described below, the colorless crystals of $BiSeO_3Cl$ exhibited an intensive SH signal that unambiguously indicated the noncentrosymmetricity of their structure. The cell parameters for the red crystals of $Bi_3Se_2O_7Cl_3$ were obtained with the use of a CAD-4 (Enraf-Nonius) X-ray diffractometer. This substance appeared to belong to a tetragonal system, its lattice constants being $a = 22.670(3)$, $c = 38.38(2)$ Å. X-ray extinction rules observed for a single crystal of $Bi_3Se_2O_7Cl_3$ indicated a primitive unit cell in its structure. The absence of SH signal in the tests means the structure most likely possesses a center of symmetry. For this reason we studied in more detail the properties of $BiSeO_3Cl$.

Crystal Structure Determination of $BiSeO_3Cl$

A small piece of $BiSeO_3Cl$ crystal with linear dimensions of about 0.15 mm was used for the detailed structure

[1] To whom correspondence should be addressed. E-mail: berdonosov@inorg.chem.msu.ru. Fax: + 7-(095)-939-0998.

0022-4596/00 $35.00
Copyright © 2000 by Academic Press
All rights of reproduction in any form reserved.

TABLE 1
Crystallographic Data for $BiSeO_3Cl$

Crystal system	Orthorhombic
Space group	$P2_12_12_1$ (No. 19)
Cell constants (Å):	
a	6.353(2)
b	7.978(3)
c	8.651(4)
Z	4
Crystal dimension (mm)	less than 0.15
μ cm^{-1}	476.27
d_{calc} (g/cm^3)	5.626(6)
Radiation (Mo$K\alpha$)	0.71069 Å
Data collection temperature (K)	293
Scan mode	ω–θ
θ max	28°
No. of measured reflections	677
No. of reflections used with $F > 4\sigma(F)$	634
No. of variables	41
Goodness of fit	1.138
RF	5.60
wR^a	15.37
Final difference Fourier map max. and min. peaks (e·Å^{-3})	6.84 and − 5.79

[a]Weighting scheme: $w = 1/\sigma^2(F^2_{obs}) + (0.0865P^2) + 20.29P)$, where $P = (\mathrm{Max}(F^2_{obs}, 0) + 2F^2_{calc}/3)$.

determination with an X-ray CAD-4 diffractometer. Twenty-four well-centered reflexes in angle intervals from 16.6 to 18 Θ-degrees were used for accurate cell dimension elaboration. The ω–Θ scanning at room temperature was performed for data collection in 1/8 of the sphere up to 28%. The X-ray data were corrected by Lorentz and polarization factors. Amendment of the data on sample absorption was applied for the basis of azimuthal scanning of five reflection with angles χ near 90°. More complete information about the experimental procedure for $BiSeO_3Cl$ crystal structure determination is presented in Table 1.

Analysis of our X-ray data for systematically absent reflections revealed only one possible noncentrosymmetric space group for the $BiSeO_3Cl$ crystal, $P2_12_12_1$. The MULTAN program from the CSD (6) software package was used for direct method solution. In this space group,

TABLE 2
Positional and Thermal Parameters for $BiSeO_3Cl$

Atom	*x*	*y*	*z*	U_{eq} (Å^2)
Bi	0.5408 (2)	1.1905 (1)	0.3292 (1)	0.0113 (4)
Se	0.8572 (4)	0.9027 (3)	0.4473 (3)	0.0112 (6)
Cl	0.2378 (1)	0.977 (1)	0.149 (1)	0.018 (1)
O1	0.654 (4)	0.879 (3)	0.958 (2)	0.015 (4)
O2	0.631 (4)	0.887 (3)	0.349 (3)	0.019 (4)
O3	0.772 (3)	0.846 (3)	0.627 (2)	0.012 (4)

TABLE 3
Anisotropic Thermal Parameters for Heavy Atoms

Atom	U_{11} (Å)	U_{22} (Å)	U_{33} (Å)	U_{23} (Å)	U_{13} (Å)	U_{12} (Å)
Bi	0.0095 (6)	0.0119 (6)	0.0125 (6)	0.0002 (3)	0.0004 (4)	0.0011 (4)
Se	0.009 (1)	0.011 (1)	0.014 (1)	0.001 (1)	− 0.002 (1)	0.001 (1)
Cl	0.009 (3)	0.016 (3)	0.028 (4)	0.002 (3)	0.001 (3)	0.002 (2)

$P2_12_12_1$, a model was found for all heavy atom arrangement with $R \leq 15\%$. In the next step, difference Fourier cycling was applied to find all the remaining atoms. The final solution was obtained using the SHELX93 program for PC computers (7) while the DIFABS program was applied for a semiempirical absorption correction. Positional and anisotropic thermal parameters obtained in the final least-squares refinement are listed in Tables 2 and 3; interatomic distances are presented in Table 4.

We encountered two problems in the course of our careful examination of $BiSeO_3Cl$ crystal structure. The first one is connected to the high positive and negative peaks we have observed on the Fourier difference map for our $BiSeO_3Cl$ crystal (Table 1). The peaks are located near bismuth atoms. This problem seems to be as yet unsolved though a similar phenomenon has been observed earlier, in the course of an X-ray study of $\beta - Bi_5O_7I$ crystal structure in (8), where high peaks of electron density on the Fourier difference map

TABLE 4
Interatomic Distances (Å) and Bond Angles within Bi and Se Polyhedra for $BiSeO_3Cl$

Bond	Distance	Bond	Distance
Bi–Se	3.218 (3)	Bi–O2	2.46 (2)
Bi–Cl	2.690 (7)	Bi–O3	2.14 (2)
Bi–Cl	3.009 (7)	Se–O1	1.75 (2)
Bi–O1	2.68 (2)	Se–O2	1.67 (2)
Bi–O1	2.30 (2)	Se–O3	1.71 (2)
Bi–O2	2.49 (2)		
Bond angle	**Angle (°)**	**Bond angle**	**Angle (°)**
O2–Se–O3	99.7 (10)	O2–Bi–O1	127.0 (7)
O2–Se–O1	93.7 (10)	O3–Bi–Cl	83.2 (6)
O3–Se–O1	101.9 (10)	O1–Bi–Cl	74.3 (5)
O3–Bi–O1	83.9 (8)	O2–Bi–Cl	74.6 (6)
O3–Bi–O2	79.6 (7)	O2–Bi–Cl	134.3 (6)
O1–Bi–O2	146.2 (8)	O1–Bi–Cl	73.5 (5)
O3–Bi–O2	78.3 (7)	O3–Bi–Cl	81.7 (6)
O1–Bi–O2	62.5 (7)	O1–Bi–Cl	130.8 (5)
O2–Bi–O2	140.0 (5)	O2–Bi–Cl	75.6 (6)
O3–Bi–O1	153.7 (7)	O2–Bi–Cl	68.5 (6)
O1–Bi–O1	101.0 (4)	O1–Bi–Cl	112.3 (5)
O2–Bi–O1	82.5 (6)	Cl–Bi–Cl	148.5 (2)

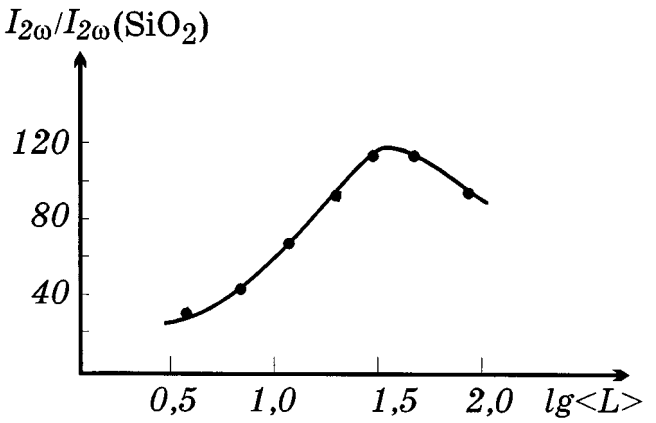

FIG. 1. Particle-size dependence of second-harmonic intensity in α-quartz units for $BiSeO_3Cl$ powders.

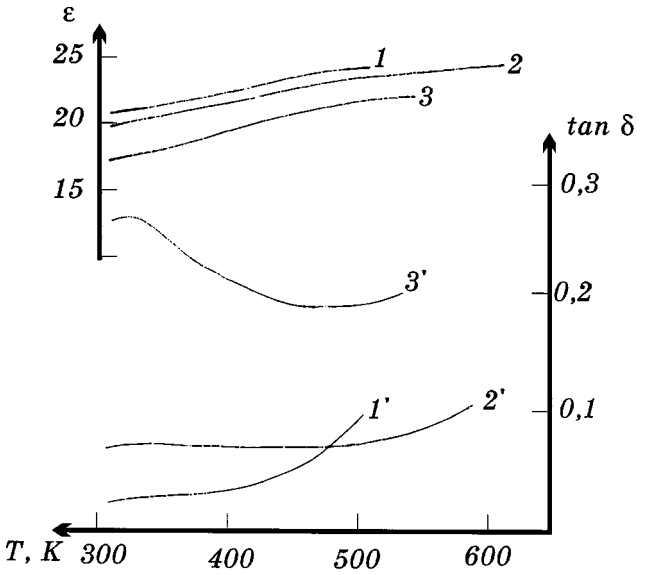

FIG. 3. Dielectric constant (ε) and loss tangent (tan δ) for a $BiSeO_3Cl$ single crystal at frequencies 1000 (1, 1′), 100 (2, 2′), and 10 kHz (3, 3′).

near Bi atoms are also clearly defined. Another problem arises from the too- large difference between the two forms of *R*-factor (*RF* and w*R*) in Table 1. We tried to explain this discrepancy as due to inadequate absorption correction for some directions. Nevertheless, analysis of 50 peaks with maximum differences between calculated and observed intensities failed to make the problem more clear.

Nonlinear Optical Properties Characteristics of $BiSeO_3Cl$

The nonlinear optical properties of $BiSeO_3Cl$ were tested by the SHG method using graded powder samples. The powders were obtained by crushing single crystals and separating the product into fractions on sieves according to particle size in powder samples. The YAG : Nd-laser was used as a source of powerful impulse radiation at wavelength $\lambda_\omega = 1.064$ μm with a repetition rate of 4 impulses per second and a duration of impulses of about 10 ns. The intensity $I_{2\omega}$ of the signal at doubled frequency ($\lambda_{2\omega} = 0.532$ μm) registered from $BiSeO_3Cl$ powder samples in the backward direction is shown in Fig. 1 in relation to the $I_{2\omega}$ of α-quartz 3-μm powder as a standard. The temperature dependencies of $I_{2\omega}/I_{2\omega}$ (SiO_2) for the powders are presented in Fig. 2.

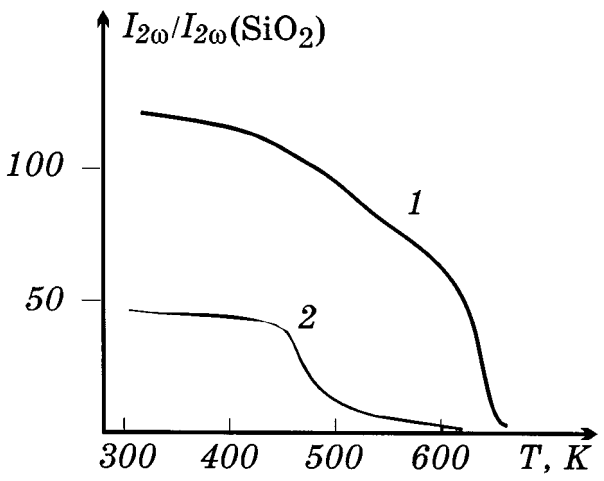

FIG. 2. Temperature dependencies of second-harmonic intensity in α-quartz units for $BiSeO_3Cl$ powder samples with particle sizes 30 μm (1) and 3 μm (2).

Dielectric Measurements

In order to characterize the dielectric properties of $BiSeO_3Cl$, a single crystal was chosen that possessed good optical quality and well-developed natural faces. Electrodes of colloidal silver were put by brush on the {011} faces of this crystal. Dielectric measurements were performed with computer-controlled *ac*-bridges R5083 and E7-12 at the electric field frequencies 10, 100, and 1000 kHz. The temperature interval of measurements from 290 to 600 K was limited from above by thermal decomposition of the crystal at ≈ 610 K. Fully reproducible in a "heating–cooling" cycle between 290 and 600 K, dielectric constant (ε) and dielectric losses tangent (tan δ) *versus* temperature curves were obtained (Fig. 3). Temperature dependencies of the specific electrical conductivity σ of $BiSeO_3Cl$ for selected electric field frequencies are given in Fig. 4.

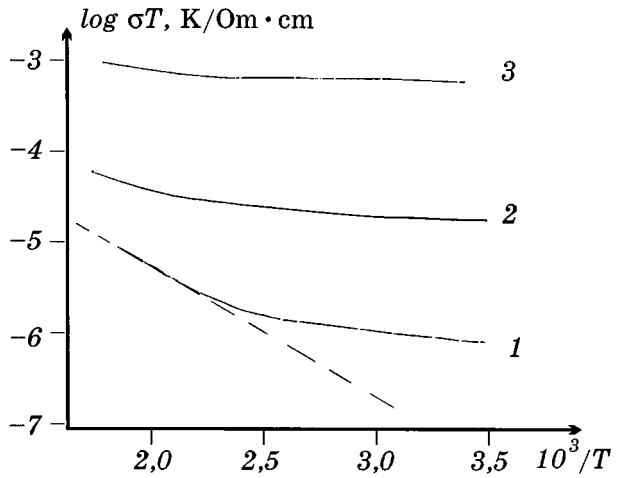

FIG. 4. The relationship between $\log \sigma T$ (σ, electric conductivity) and reciprocal temperature for a $BiSeO_3Cl$ single crystal along the {011} direction at frequencies 10 (1), 100 (2), and 1000 (3) kHz.

RESULTS AND DISCUSSION

Projections of the $BiSeO_3Cl$ crystal structure on different crystallographic planes are shown in Fig. 5.

The nearest coordination surroundings of Bi atoms (50 + 1Cl, Table 4) form a distorted octahedron. An additional chlorine atom at a distance of 3.009(7) Å constructs a distorted pentagonal bipyramid (Fig. 6). Interatomic distances Bi–O and Bi–Cl are typical for bismuth compounds. For example in the α-Bi_2O_3 structure the Bi–O distance lies in the range 2.133–2.787 Å (9), and $BiCl_3$ the Bi–Cl distance to the nearest chlorine atoms is 2.5 Å, and for second coordination surroundings—3.2 Å (10).

The nearest surroundings of selenium atoms in $BiSeO_3Cl$ are usual for the Se(IV) compounds in which three oxygen atoms are tightly connected with the selenium atom (Table 4). Such "opened" polyhedra are rather typical for the cations possessing a lone pair of electrons. Thus, the selenium coordination polyhedron is usually described as the SeO_3E tetrahedron.

The BiO_5Cl_2 polyhedra described above are connected by Cl–O edges and form zig-zag chains parallel to the *b* axis. Each BiO_5Cl_2 polyhedron is linked by common oxygen vertices with two BiO_5Cl_2 polyhedra from different chains. From each pair of BiO_5Cl_2 polyhedra in a chain, one BiO_5Cl_2 polyhedron is connected to two different chains, and the other one is connected to another two chains. Each $[BiO_5Cl_2]_\infty$ chain is connected to the four nearest chains of $[BiO_5Cl_2]_\infty$ (Fig. 7).

SeO_3E pyramids are connected to BiO_5Cl_2 polyhedra by oxygen edges from a BiO_5Cl_2 polyhedron from one chain and by one oxygen vertex from a BiO_5Cl_2 polyhedron from another chain.

The crystal structure of $BiSeO_3Cl$ is different from isoformula $BiTeO_3X$ (X = Br, I) compounds, which are layered Sillen phases, described in the Introduction.

It is interesting to evaluate second-order optical nonlinearly for noncentrosymmetric $BiSeO_3Cl$ crystals. In accordance with (12, 13) for the angular average second-order polarizability tensor $\langle d \rangle$, the simple expression in [3] should be valid under the condition that coherence length

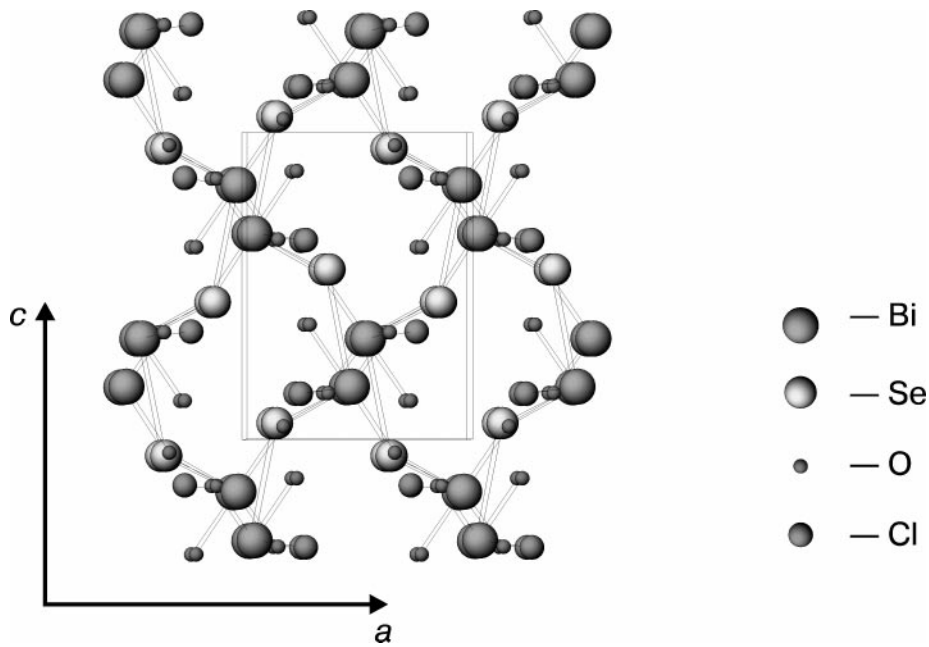

FIG. 5. $BiSeO_3Cl$ crystal structure, projection on the *ac* plane.

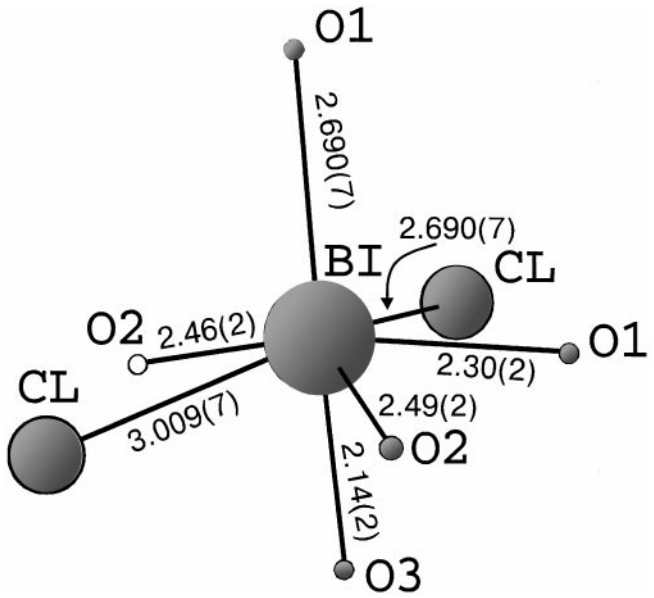

FIG. 6. Coordination surroundings for the Bi atom in $BiSeO_3Cl$.

l_c is much larger in comparison to particle size $\langle L\rangle = 3\ \mu m \ll l_c$ in the powder sample,

$$\langle d\rangle = A \cdot d_{11}(q) \cdot [(n+1)/(n_q+1)]^3 \cdot [I_{2\omega}/I_{2\omega}(q)]^{1/2}, \quad [3]$$

where $d_{11}(q) = 0.36 \times 10^{-12}$ m/V is the nonlinear coefficient for α-quartz, n and n_q are the refractive indices for the sample under investigation and quartz, $I_{2\omega}$ and $I_{2\omega}(q)$ are second harmonic intensities for the sample and quartz, respectively, and A is a geometrical coefficient close to unity. The condition $L \ll l_c$ is surely the case for thin $BiSeO_3Cl$ powders as can be seen in Fig. 1. Indeed, the dependence of second harmonic intensity upon the average size of particles L of a powder sample has a maximum at $L \approx 35\ \mu m$ (Fig. 1). Based on consideration of Kurtz and Dougherty (12), this value is exactly l_c—the length of the so-named coherent interaction between Nd-laser radiation and its second harmonic. The observed value of l_c in $BiSeO_3Cl$ is too small and does not meet the requirements for effective frequency doubling of Nd-laser radiation ($l_c > 1$ cm) though the $BiSeO_3Cl$ crystal may be useful for other nonlinear optics applications, such as noncollinear mixing of frequencies. Taking into account that under the $L \ll l_c$ condition (Fig. 1) $I_{2\omega}/I_{2\omega}(SiO_2) = 25$ and accepting for n the typical value ≈ 2.2 we obtain $\langle d\rangle \approx 10 d_{11}(q) = 3.6 \times 10^{-12}$ m/V. This value is rather high and close to the second-order optical nonlinearly of the well-known Bi-containing oxide ferroelectric Bi_2WO_6 (14).

The temperature dependencies of nonlinear optical response of $BiSeO_3Cl$ powders (Fig. 2) give more information about changes of the optical and chemical properties of $BiSeO_3Cl$ on heating. Strong dependence of $I_{2\omega}$ on temperature between 290–450 K for coarse powder (curve 1 in Fig. 2) roughly reflects $l_c(T)$ behavior. In contrast, in the thin powder case ($L \sim 3\ \mu m$) l_c has no influence on $I_{2\omega}$, as is seen in curve 2 (Fig. 2) up to 450 K. Above the limit of 450 K, irreversible fade-outs of the nonlinear response are clearly marked in curve 2 and to a lesser degree in curve 1. The more developed surface of thinner powder favors demolition of the nonlinear properties of the sample. The reason is oxidation by air beginning at 450 K. The final vanishing of the second harmonic signal at 610 K does not depend on the particle size of the sample but corresponds to chemical decomposition in the bulk of the substance. So on the basis of SHG data it can be concluded that apart from the oxidation process on the surface above 450 K, the noncentrosymmetric phase of $BiSeO_3Cl$ is stable up to 610 K, where it decays to SeO_2 and BiOCl, as both chemical analysis and thermal analysis confirm.

The absence of distinct anomalies in the temperature dependencies of the dielectric constant (ε) and the dielectric losses ($\tan\delta$) indicates that no phase transitions in $BiSeO_3Cl$ single crystals occur in the interval 293–610 K. The low value of ε and its small change with temperature are in accordance with there being no polar domains in $BiSeO_3Cl$ and help exclude the possibility of ferroelectricity above room temperature. At the same time, the regular lowering of the dielectric constant with frequency (Fig. 3) reveals some

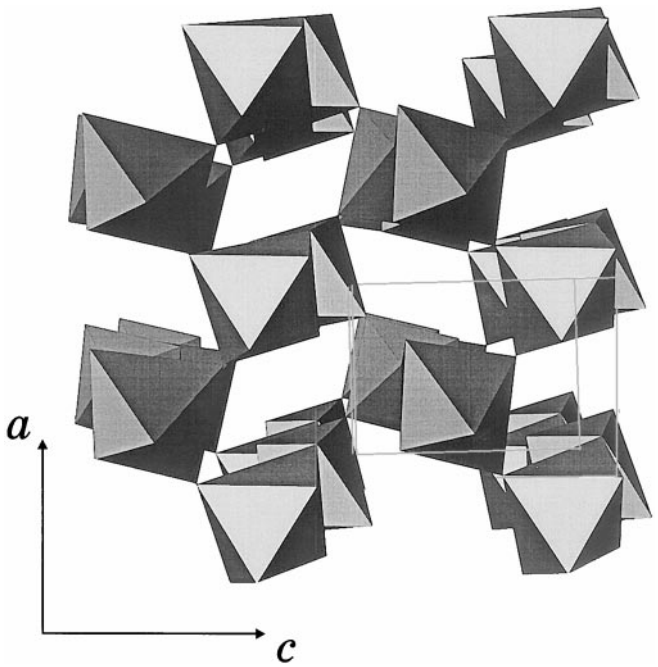

FIG. 7. $[BiO_5Cl_2]_\infty$ chains in $BiSeO_3Cl$. The unit cell is marked.

dielectric relaxation due to ions jumping over the vacancies in the crystal lattice. As the result of this motion, ionic conductivity (σ), presumably oxygen in nature, may be supposed to take place in $BiSeO_3Cl$, similar to many other bismuth oxides. If so, the dependence of the conductivity upon frequency (ω) must obey the usual law,

$$\sigma = \sigma_0\ [1 + (\omega/\omega_j)^p], \qquad [1]$$

where σ_0 is direct current conductivity, ω_j is ion jump frequency, and p is a coefficient less than or equal to 1 (11). Approximation with Eq. [1] of the experimental data in Fig. 4 and extrapolation of these data to zero frequency at $T = 300\,K$ leads to the relatively small value $\sigma_0 \approx 10^{-9}$–$10^{-10}\,Om^{-1}\,cm^{-1}$. Dielectric relaxation in $BiSeO_3Cl$ at low temperature prevents characterization of ionic conductivity by means of an Arrhenius-type interrelation:

$$\sigma_0(T) = \text{const.}\ \exp(-E/k_BT). \qquad [2]$$

Taking into consideration only the high-temperature part of $\log \sigma T(1/T)$ curve in Fig. 2 at frequency 10 kHz for activation energy determination, we come to $E_a = 0.3$–$0.4\,eV$, which seems to be reasonable for oxygen ion mobility. As the dielectric relaxation observed in $BiSeO_3Cl$ strongly implies that vacancies are involved in these transport phenomena, new questions arise about the nature of these vacancies and their possible relations to bismuth lone-pair behavior. More precise X-ray studies are necessary to answer such questions and to clear up the structural mechanism of ion conductivity in $BiSeO_3Cl$.

ACKNOWLEDGMENTS

We thank Drs. O.G. D'yachenko and A.V. Shevelkov from MSU for their help with the X-ray structure analysis. We are grateful to Dr. P. Lightfoot, University of St. Andrew, for taking part in discussions. This work was partially supported by INTAS program grant INTAS 96-1324.

REFERENCES

1. M. B. Novikova, V. A. Dolgikh, L. N. Kholodkovskaya, S. Yu. Stefanovitch, and A. E. Baron, *MSU Bull. Chem.* **45**(1), 59 (1990).
2. I. V. Tarasov, V. A. Dolgikh, B. A. Popovkin, and A. E. Baron *Russ. J. Inorg. Chem.* **40**(1), 139 (1995).
3. L. N. Kholodkovskaya, V. A. Dolgikh, and B. A. Popovkin, *Russ. J. Inorg. Chem.* **36,** 1244 (1991).
4. L. N. Kholodkovskaya, V. A. Dolgikh, and B. A. Popovkin, *J. Solid State Chem.* **116,** 406 (1995).
5. V. A. Dolgikh, L. N. Kholodkovskaya, and B. A. Popovkin, *Russ. J. Inorg. Chem.* **41,** 932 (1996).
6. L. G. Akselrud, Yu. N. Gyn, P. Yu. Zavalij, V. K. Pecharsky, and V. S. Fumdamentsky, "Thes. Report on 12th ECM," p. 155, Moscow, 1989.
7. G. M. Sheldrick, "SHELXL-93, Program for Crystal Structure Refinement," Universität Göttingen, 1993.
8. J. Ketterer, E. Keller, and V. Kromer, *Z. Kristallogr.* **172,** 63 (1985).
9. H. A. Harwig, *Z. Anorg. Allg. Chem.* **444,** 151 (1978).
10. S. C. Nuburg, J. A. Ozin, and J. T. Seymanski, *Acta Crystallogr.* **B27,** 2298 (1971).
11. S. Yu. Stefanovitch, L. A. Ivanova, and A. V. Astafiev, "Ionic and Superionic Conductivity in Ferroelectrics," pp. 80–120. NIITEKhim, Moscow, 1989. [Review].
12. S. K. Kurtz and J. P. Dougherty, "Syst. Mater. Anal." Vol. 4, pp. 269–337. New York, 1978.
13. S. Yu. Stefanovich, *in* "Europ. Conf. on Lasers and Electro-Optics (CLEO-Europe'94), Amsterdam, 1994," abstracts, pp. 249–250.
14. S. K. Kurtz and T. T. Perry, *J. Appl. Phys.* **39,** 3798 (1968).